

Portrait3D: Text-Guided High-Quality 3D Portrait Generation Using Pyramid Representation and GANs Prior

YIQIAN WU, State Key Lab of CAD&CG, Zhejiang University, China
 HAO XU, State Key Lab of CAD&CG, Zhejiang University, China
 XIANGJUN TANG, State Key Lab of CAD&CG, Zhejiang University, China
 XIEN CHEN, Yale University, United States of America
 SIYU TANG, ETH Zürich, Switzerland
 ZHEBIN ZHANG, OPPO US Research Center, United States of America
 CHEN LI, OPPO US Research Center, United States of America
 XIAOGANG JIN*, State Key Lab of CAD&CG, Zhejiang University, China



Fig. 1. Using text as input, our text-to-3D-portrait method, Portrait3D, can automatically generate a variety of realistic textured 3D portraits. Portrait3D consistently produces high-quality 3D portraits that are aligned with the provided text prompts. Each portrait is rendered from eight different views using volume rendering.

Existing neural rendering-based text-to-3D-portrait generation methods typically make use of human geometry prior and diffusion models to obtain guidance. However, relying solely on geometry information introduces issues such as the Janus problem, over-saturation, and over-smoothing. We present *Portrait3D*, a novel neural rendering-based framework with a novel joint geometry-appearance prior to achieve text-to-3D-portrait generation that overcomes the aforementioned issues. To accomplish this, we train a 3D portrait generator, 3DPortraitGAN \clubsuit , as a robust prior. This generator is capable of producing 360° canonical 3D portraits, serving as a starting point for the subsequent diffusion-based generation process. To mitigate the “grid-like” artifact caused by the high-frequency information in the feature-map-based 3D representation commonly used by most 3D-aware GANs, we integrate a novel *pyramid tri-grid* 3D representation into 3DPortraitGAN \clubsuit . To generate 3D portraits from text, we first project a randomly generated image aligned with the given prompt into the pre-trained 3DPortraitGAN \clubsuit ’s latent space. The resulting latent code is then used to synthesize a *pyramid tri-grid*. Beginning with the obtained *pyramid tri-grid*, we use score distillation sampling to distill the diffusion model’s knowledge into the *pyramid tri-grid*. Following that, we utilize the diffusion model to refine the rendered images of the 3D portrait and then use these refined images as training data to further optimize the *pyramid tri-grid*, effectively eliminating issues with unrealistic color and unnatural artifacts. Our experimental results show that Portrait3D can produce realistic, high-quality, and canonical 3D portraits that align with the prompt.

*Corresponding author.

CCS Concepts: • **Computing methodologies** → **Computer vision**.

Additional Key Words and Phrases: 3D portrait generation, 3D-aware GANs, diffusion models

1 INTRODUCTION

3D portrait modeling can benefit from neural rendering techniques, such as NeRF [Mildenhall et al. 2020], NeuS [Wang et al. 2021], and Gaussian Splatting [Kerbl et al. 2023a], due to their powerful ability to represent detailed shapes and produce realistic rendering results. The introduction of the diffusion model [Ho et al. 2020] and score distillation sampling (SDS) [Poole et al. 2023] has further spurred the rapid development of text-to-3D-portrait generation by distilling the knowledge of 2D image prior into 3D representation. To obtain shape guidance, diffusion-based 3D portrait generation can leverage human geometry prior information, including SMPL [Loper et al. 2015] (and its variants), FLAME [Li et al. 2017], DensePose [Güler et al. 2018], and imGHUM [Alldieck et al. 2021].

Existing methods, however, primarily use geometric priors as initial points for generation in order to establish shape constraints, with the diffusion model providing all appearance information. This can result in issues like inconsistent or unrealistic textures. Furthermore, applying SDS to a coarse initialization can lead to over-saturation and over-smoothing. As a result, a robust joint geometry-appearance

prior is still required to achieve realistic and high-quality 3D portrait generation. The key challenge in accomplishing this is the requirement for the prior to include full-head geometry-appearance information while also having the expressive power to portray a diverse range of 3D portraits.

In this paper, we present *Portrait3D*, a neural rendering-based framework to generate high-quality and realistic 3D portraits following the input prompt. *Portrait3D* utilizes novel joint geometry-appearance prior information from 3D-aware GANs and guidance from the diffusion model. However, performing score distillation sampling directly on the feature-map-based 3D representation used by many 3D-aware GANs can result in the “grid-like” artifact, which is caused by underlying exclusive high-frequency information. To address this, we propose 3DPortraitGAN \triangle , a 3D portrait generator utilizing a novel *pyramid tri-grid* 3D representation to effectively alleviate the “grid-like” artifact. The symbol “ \triangle (pyramid)” indicates the usage of a pyramid-structure representation. 3DPortraitGAN \triangle is capable of producing 360° canonical 3D full-head portraits and providing a prior for our framework. During the process of text-to-3D-portraits generation, given a text prompt, we first randomly generate a portrait image by feeding the text prompt into the diffusion model, and then project the generated image into the latent space of our generator. The resulting latent code is used to synthesize the corresponding *pyramid tri-grid*, which serves as the starting point of the subsequent diffusion-based generation process. Following that, we distill the knowledge of the diffusion model into the *pyramid tri-grid* through score distillation sampling. This process produces a 3D portrait that aligns with the input prompt. To further enhance the quality of the obtained 3D portrait, we apply the diffusion model to process its rendered images. The refined rendered images are then used as training data to optimize the *pyramid tri-grid*, yielding the final results.

Through comprehensive experiments, we demonstrate that *Portrait3D* is capable of generating high-quality, view-consistent, realistic, and canonical 3D portraits that align well with the input text prompt. Notably, our generation pipeline requires only a graphics card with 12GB of memory.

In summary, our work makes the following major contributions:

- A 3D portrait generator that employs a novel *pyramid tri-grid* 3D representation to mitigate the “grid-like” artifact, and learns a distribution of 360° canonical 3D portraits to serve as a robust prior for our framework.
- A text-to-3D-portrait generation framework, *Portrait3D*, leverages prior information from our 3D portrait generator and guidance from the diffusion model, producing high-quality, view-consistent, realistic, and canonical 3D portraits that are in alignment with the input text prompts.

2 RELATED WORK

2.1 3D-aware GANs

Ever since Goodfellow et al.’s groundbreaking innovation of Generative Adversarial Networks (GANs) [Goodfellow et al. 2014] in 2014, a multitude of GAN models [Gulrajani et al. 2017; Karras et al. 2018; Radford et al. 2016] have been proposed, yielding impressive outcomes in the domain of photorealistic image synthesis. Over

recent years, 2D generators have been extended by incorporating voxel rendering [Nguyen-Phuoc et al. 2020; Zhu et al. 2018] or NeRF rendering [Chan et al. 2021; Gu et al. 2022] with the generative network backbone, achieving view-consistent image generation and catalyzing the emergence of 3D-aware GANs. A number of effective optimization strategies and frameworks [Chen et al. 2023a; Skokhodov et al. 2022; Trevithick et al. 2024] have been developed to facilitate the generation of high-resolution outcomes, eliminating the necessity for a super-resolution module. The endeavor to reconstruct 3D faces from input images using 3D-aware generators has spurred the development of inversion techniques [Ko et al. 2023; Trevithick et al. 2023; Xie et al. 2023; Yin et al. 2023]. This progression has enhanced the manipulation of real images and videos.

The 3D representations within 3D-aware GANs can be parameterized using coordinate-based networks [Chan et al. 2021; Gu et al. 2022], feature maps [An et al. 2023; Chan et al. 2022], signed distance fields (SDF) [Gao et al. 2022], radiance manifolds [Wu et al. 2023b], or voxel grids [Schwarz et al. 2022; Zhu et al. 2018]. The feature-map-based 3D representation, known as *tri-plane*, was first introduced in EG3D [Chan et al. 2022]. Since then, it has become a widely adopted 3D representation that has been extensively utilized and expanded upon by numerous 3D-related works [An et al. 2023; Chen et al. 2023a; Gao et al. 2022; Sun et al. 2022; Wang et al. 2023b; Yi et al. 2023; Zhang et al. 2023b].

However, most 3D-aware face GANs utilize datasets mainly comprising frontal or near-frontal views, such as *FFHQ* and *CelebA*. This leads to incomplete head geometry, making these generators unsuitable to serve as 3D portrait generation priors. *PanoHead* [An et al. 2023], trained on *FFHQ-F*, is designed to generate full-head results using an innovative *tri-grid* representation. The *tri-grid* representation is derived from *tri-plane*, and is designed to eliminate the “mirrored face” artifacts. However, given that *FFHQ-F* solely encompasses the head region, *PanoHead*’s generation is similarly restricted, resulting in a lack of complete geometry of neck and shoulder areas. 3DPortraitGAN [Wu et al. 2023a] further pushes the boundaries in this direction, facilitating 3D one-quarter headshot generation (including the head, neck, and shoulders). This is achieved by constructing a novel 360° *PHQ* dataset, incorporating mesh-guided deformation, and implementing body pose self-learning.

2.2 Diffusion-based 3D Portrait Generation

Since the advent of the Diffusion Model [Ho et al. 2020], it has emerged as a crucial tool for 2D image generation. Stable Diffusion [Rombach et al. 2022], also known as the latent diffusion model, further expands the diffusion model to the latent space of a pre-trained autoencoder model, significantly reducing computational costs while maintaining the quality of generation. However, training a diffusion model requires substantial amounts of training data, posing challenges for 3D content generation due to the difficulty in obtaining 3D data. To bridge this gap between 2D and 3D space, DreamFusion [Poole et al. 2023] introduces a novel method known as Score Distillation Sampling (SDS). SDS seeks to optimize the parameters of a differential renderer by penalizing the discrepancy

between the predicted noise and the noise added to the rendered image, aiming to make the rendered image align with the image distribution learned by the diffusion model. ProlificDreamer [Wang et al. 2023a] introduces Variational Score Distillation (VSD), which treats the 3D scene given a textual prompt as a random variable instead of a single point, effectively alleviating issues of over-saturation, over-smoothing, and low diversity encountered in SDS.

By adapting general diffusion-based text-to-3D techniques to portrait-specific designs, text-to-3D portrait generation has become a popular research topic. Some methods employ meshes and textures to represent 3D portraits [Liao et al. 2023; Xu et al. 2023b; Zhang et al. 2023a], and these generation methods can be accomplished by first deforming parametric body shape models and then generating corresponding textures. However, these methods face challenges in generating realistic results. Neural implicit representation [Kerbl et al. 2023a; Mildenhall et al. 2020; Wang et al. 2021], on the other hand, can represent detailed shapes and produce realistic results, making it a popular 3D portrait representation. Since the inception of 3D Gaussian Splatting [Kerbl et al. 2023b], it has emerged as a popular representation of 3D portraits, capable of achieving real-time rendering. This method has been employed in portrait reconstruction studies [Chen et al. 2023b; Rivero et al. 2024; Wang et al. 2024; Xu et al. 2023a], as well as in text-to-3D-portrait generation [Zhou et al. 2024]. Because human faces and bodies exhibit strong regularity, prior information can be extracted from a variety of human data sources to guide diffusion-based 3D portrait generation. A stream of research employs body shape models, such as SMPL [Hu et al. 2023; Jiang et al. 2023], FLAME [Han et al. 2023], imGHUM [Kolotouros et al. 2023], as the initial point for text-to-3D-portrait generation. 3D avatars can also be generated from reference images [Albahar et al. 2023; Ho et al. 2023; Huang et al. 2023b] by utilizing the diffusion model to generate unseen regions with seamless integration, which can be guided by a human body shape prediction network [Albahar et al. 2023] or a back appearance hallucinator and normal predictor [Ho et al. 2023]. Research efforts have also been directed towards editing 3D objects, including 3D portraits, utilizing the diffusion model [Haque et al. 2023].

Nonetheless, the necessity for a robust joint geometry-appearance prior persists. Exclusively considering geometry information leads to issues such as inconsistent or unrealistic texture. Additionally, implementing SDS on a coarse initialization can engender over-saturation and over-smoothing. In this paper, we propose using 3D-aware GANs as a robust prior, which learns the joint distribution of portrait geometry and texture, thereby enhancing the process of 3D portrait generation.

3 METHODOLOGY

3.1 Overview

In this section, we present an overview of Portrait3D. We first introduce our novel 3D representation named *pyramid tri-grid* in Sec. 3.2. This representation incorporates multiple-resolution features and aids in alleviating the “grid-like” artifact that occurs during score distillation sampling. In Sec. 3.3, we describe our 3D-aware generator, 3DPortraitGAN[▲]. This generator incorporates a 3D-aware branch into the original 2D StyleGAN backbone, allowing

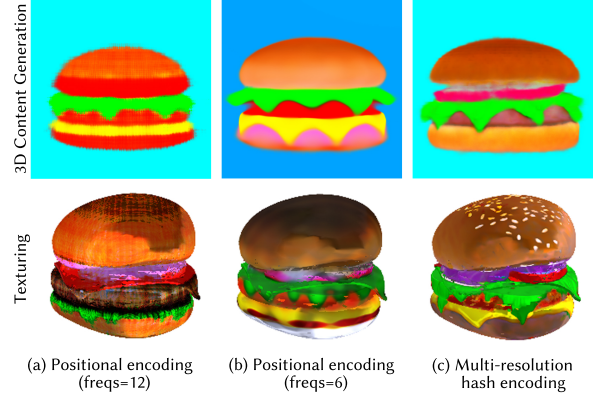


Fig. 2. The results of score distillation sampling for 3D content generation (top) and texture generation (bottom), using positional encoding with a different number of frequencies (a,b), and multi-resolution hash encoding (c). The same prompt, “a hamburger”, was used for a fair comparison.

3DPortraitGAN[▲] to output the *pyramid tri-grid* and furnish prior information for the subsequent process. Next, in Sec. 3.4, we propose a novel text-guided 3D portrait generation algorithm. Leveraging the prior information provided by 3DPortraitGAN[▲], this algorithm produces 3D portraits via score distillation sampling. Lastly, in Sec. 3.5, we elaborate on the final procedure to further enhance the quality of 3D portraits. We adopt a diffusion model to refine the rendered images and utilize them to optimize the 3D portrait.

3.2 Pyramid Tri-grid

3DPortraitGAN [Wu et al. 2023a] is a 3D-aware generator capable of generating 3D full-head avatars, and can function as a prior for 3D portrait generation. 3DPortraitGAN draws inspiration from Panohead [An et al. 2023] and utilizes a feature-map-based 3D representation named *tri-grid* (we denote it as $T \in \mathbb{R}^{3 \times 3 \times 32 \times 256 \times 256}$) to store the features of color and density of a 3D portrait.

During the neural rendering process, the *tri-grid* is processed through a neural renderer to produce RGB images:

$$x_{rgb} = R(T, c, w), \quad (1)$$

where R is the neural renderer, c denotes the camera parameters, and w denotes the latent code. The *tri-grid* is first rendered to a feature image $x_{feature}$ via volume rendering. Specifically, a point x is sampled on the ray and then projected onto the *tri-grid* to query features, which are aggregated through summation and then input into a decoder to predict the color features and density required for volume rendering. Next, a ToRGB module, modulated by the latent code w , converts $x_{feature}$ into the RGB image x_{rgb} .

A straightforward 3D portrait generation approach might involve directly applying score distillation sampling to the *tri-grid* generated by the 3DPortraitGAN, which already stores the information of a coarse 3D portrait. However, this results in significant “grid-like” artifacts (detailed in Sec. 6.1). We attribute this phenomenon to the exclusive high-frequency information encoded in the single-resolution *tri-grid* representation.

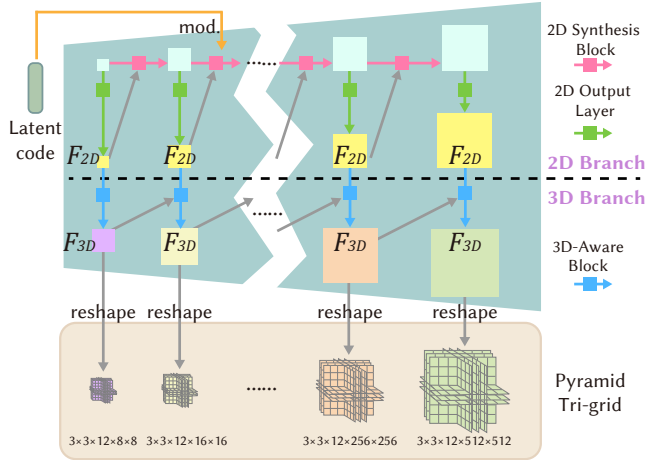


Fig. 3. The architecture of the 3D-aware *pyramid tri-grid* generator in 3DPortraitGAN[▲]. The *pyramid tri-grid* is composed of *tri-grids* generated at different layers. For the sake of simplicity and clarity, we omit the latent code modulation applied to each block.

We conducted a simple example to demonstrate our intuition, as shown in Fig. 2. Score distillation sampling was used in this experiment for two tasks: (1) 3D content generation¹ and (2) generating texture for a given mesh², with the prompt “a hamburger.” To facilitate the representation of high-frequency content, we used the positional encoding strategy [Mildenhall et al. 2020]. As shown in Fig. 2 (a), positional encoding causes “grid-like” artifacts. We then investigated two methods to mitigate the effect of high-frequency information: reducing the maximum frequency of positional encoding from 12 to 6 (Fig. 2 (b)) and employing multi-resolution hash encoding [Müller et al. 2022] (Fig. 2 (c)). Both methods successfully reduce “grid-like” artifacts. Owing to its multi-resolution structure, hash encoding could achieve a better balance between generating highly detailed results and mitigating high-frequency noise.

Inspired by multi-resolution hash encoding, we introduce a novel 3D representation named *pyramid tri-grid*, which incorporates a similar multi-resolution pyramid structure by encompassing *tri-grids* of different resolutions: {8, 16, 32, 64, 128, 256, 512}. During feature querying, features on *tri-grids* of different resolutions are aggregated through summation. We find that a channel dimension of 12 offers sufficient expressive power, thereby our *pyramid tri-grid* is defined as $T^{Pyr} = [T^8 \in \mathbb{R}^{3 \times 3 \times 12 \times 8 \times 8}, \dots, T^{512} \in \mathbb{R}^{3 \times 3 \times 12 \times 512 \times 512}]$.

3.3 3DPortraitGAN[▲]

We subsequently incorporate the *pyramid tri-grid* into 3DPortraitGAN, thereby establishing it as the foundational 3D representation. We refer to this newly developed 3D portrait generator as 3DPortraitGAN[▲] (the network architecture is detailed in the supplementary file).

¹We used the stable-diffusion-2-1-base model and adopted the SDS implementation provided by <https://github.com/ashawkey/stable-dreamfusion>.

²We utilized the stable-diffusion-2-1-base model and used the “Texture phase” of Fantasia3D from <https://github.com/threestudio-project/threestudio>.

To implement the generation of multiple-resolution *pyramid tri-grid*, we propose an innovative 3D-aware *pyramid tri-grid* generator, as shown in Fig. 3. Inspired by Mimic3D [Chen et al. 2023a], we incorporate a 3D-aware branch into the original 2D StyleGAN backbone to bolster feature communications between 3D-associated positions across different feature maps. At each layer, the 2D branch outputs the feature map F_{2D} through a 2D output layer. F_{2D} is then fed into the 3D branch. Within the 3D branch, a 3D-aware block equipped with a $\times 2$ upsample operation processes F_{2D} , leading to a feature map F_{3D} . F_{3D} is then reshaped into a *tri-grid*. Additionally, F_{3D} is fed to the 3D-aware block of the succeeding 3D layer.

3.4 Diffusion-based 3D Portrait Generation

We rely on the prior information provided by our 3DPortraitGAN[▲] to initialize the text-to-3D-portrait generation process.

Specifically, as depicted in Fig. 4, given a prompt describing a particular portrait, we first generate a random portrait image I using the diffusion model, and then process I to produce an aligned image $I_{aligned}$ following the alignment setting of 3DPortraitGAN[▲]. Subsequently, we obtain the inversion latent code w^* of the aligned image through latent code optimization (detailed in the supplementary file). Then w^* is fed to the 3D-aware *pyramid tri-grid* generator to obtain a *pyramid tri-grid*:

$$T^{Pyr} = \mathcal{G}(w^*), \quad (2)$$

where \mathcal{G} denotes our 3D-aware *pyramid tri-grid* generator.

After that, we freeze the parameters of the neural renderer (as shown in Fig. 4), and employ score distillation sampling to distill the knowledge of the diffusion model into the *pyramid tri-grid*:

$$\begin{aligned} \nabla_{\theta} \mathcal{L}_{SDS}(\phi, x = R(T^{Pyr}, c, w^*)) \\ \triangleq \mathbb{E}_{t, \epsilon} \left[\omega(t) \left(\hat{\epsilon}_{\phi}(z_t; y, t) - \epsilon \right) \frac{\partial z_0}{\partial x} \frac{\partial x}{\partial \theta} \right]. \end{aligned} \quad (3)$$

Here, ϕ represents the parameters of the U-Net network $\hat{\epsilon}_{\phi}$ within the latent diffusion model, while θ denotes the parameters of the *pyramid tri-grid* T^{Pyr} . ϵ represents the random noise added to the latent z_0 . The latent z_0 is derived from the rendered RGB image $x = R(T^{Pyr}, c, w^*)$ by feeding it into the encoder of the latent diffusion model’s autoencoder. The term $\frac{\partial z_0}{\partial x}$ refers to the Jacobian of the autoencoder’s encoder, playing the role in backpropagating gradients from the latent space to the RGB space. Meanwhile, z_t represents the noisy latent at time t , obtained by adding noise to z_0 . y denotes the text embeddings. $\omega(t)$ serves as a weighting function that absorbs the constant $\alpha_t \mathbf{I} = \partial z_t / \partial z_0$. The gradient $\nabla_{\theta} \mathcal{L}_{SDS}(\phi, x = R(T^{Pyr}, c, w^*))$ is utilized to update θ .

3.5 Diffusion-based 3D Portrait Optimization

After applying score distillation sampling, the 3D portraits generated from T^{Pyr} still exhibit unnatural artifacts (refer to Sec. 6.2). To address this, we propose a method to further enhance the quality of the obtained 3D portrait.

As shown in Fig. 4, we render 21 views using T^{Pyr} . Specifically, we sample 7 uniformly distributed azimuth angles from the range $[0^\circ, 360^\circ]$. For each azimuth angle, we sample 3 elevation angles from the ranges $[55^\circ, 65^\circ]$, $[85^\circ, 95^\circ]$, and $[115^\circ, 125^\circ]$, respectively.

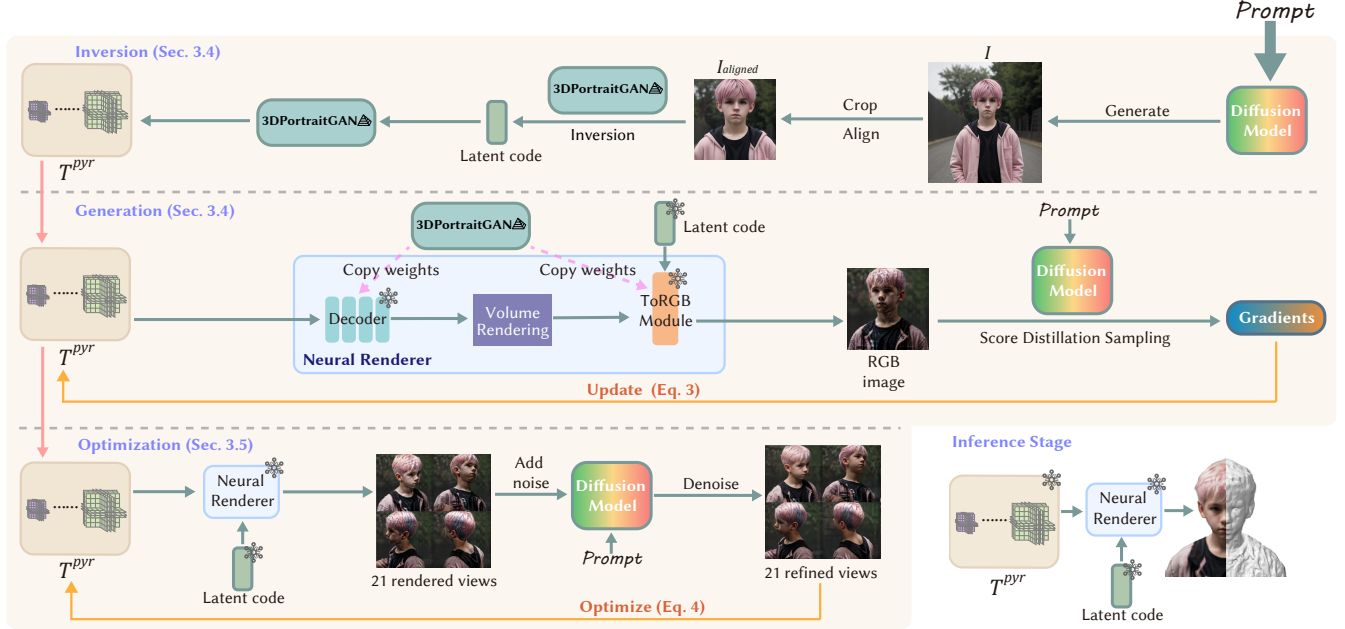


Fig. 4. The 3D portrait generation pipeline of Portrait3D. The “❄️” denotes that the submodule or representation is frozen.

These angles are then used to render 21 views by feeding T^{pyr} to the neural renderer. Subsequently, we add randomly sampled noise with a constant noise level to the rendered views, and employ the diffusion model to denoise these images. This step aims to yield high-quality views of the 3D portraits devoid of artifacts. Finally, we compute the L_2 loss between the refined views and the rendered views of T^{pyr} to optimize T^{pyr} ’s parameters θ :

$$\theta^* = \arg \min_{\theta} L_{optim} = \arg \min_{\theta} L_2(x_{refined}^c, R(T^{pyr}, c, w^*)), \quad (4)$$

where $x_{refined}^c$ denotes the refined view rendered using camera parameters c . We optimize T^{pyr} ’s parameters by penalizing the L_{optim} loss while keeping the parameters of the neural renderer unchanged, thus obtaining the final result of our framework. As depicted in Fig. 4, during the inference phase, T^{pyr} represents a high-quality 3D portrait and can generate view-consistent portrait images via the neural renderer.

4 RESULTS

4.1 Visual Results

Fig. 9 and Fig. 10 present a set of text-to-3D-portrait results generated by Portrait3D. The background for each instance is generated by the background generator in 3DPortraitGAN utilizing the inversion latent code. The results are generated in the canonical space. Considering that the results of our 3DPortraitGAN predominantly cover the upper body region, all our prompts commence with the phrase “upper body photo”. Additionally, we include terms such as “8k UHD”, “high quality”, and “cinematic” in the input prompts to facilitate the generation of more stable, high-quality images. We

omit these terms that are not directly pertinent to the semantics of 3D portraits from the figures to avoid redundancy.

The results illustrate the capability of Portrait3D to generate 3D portraits that are highly consistent with the input text. Owing to the robust prior information from 3DPortraitGAN, the generated portraits are realistic and high-quality, successfully avoiding problems such as over-saturation and the Janus problem. Moreover, Portrait3D is able to generate a diverse range of 3D portraits, encompassing various races, ages, genders, hairstyles, and so forth. More results are presented in the supplementary file.

4.2 Runtime

Portrait3D necessitates 0.5 hours on a single NVIDIA RTX 4090 GPU with 24 GB of memory to generate a 3D portrait. The image inversion process takes approximately 4 minutes. The 3D portrait generation process requires about 22 minutes. The 3D portrait optimization process consumes around 5 minutes. Portrait3D can also operate on a GPU with only 12 GB of memory, such as the NVIDIA RTX 3080Ti, with a processing time requirement of 1.5 hours. The image inversion process takes approximately 6.5 minutes. The 3D portrait generation process requires about 50 minutes. The 3D portrait optimization process consumes around 30 minutes.

5 COMPARISON

We compare our Portrait3D with text-to-3D approaches focused on general objects, such as DreamFusion [Poole et al. 2023] and LucidDreamer [Liang et al. 2023], and approaches focused on 3D portraits, such as TADA [Liao et al. 2023], AvatarCraft [Jiang et al. 2023], AvatarStudio [Zhang et al. 2023c], HumanGaussian [Liu et al.

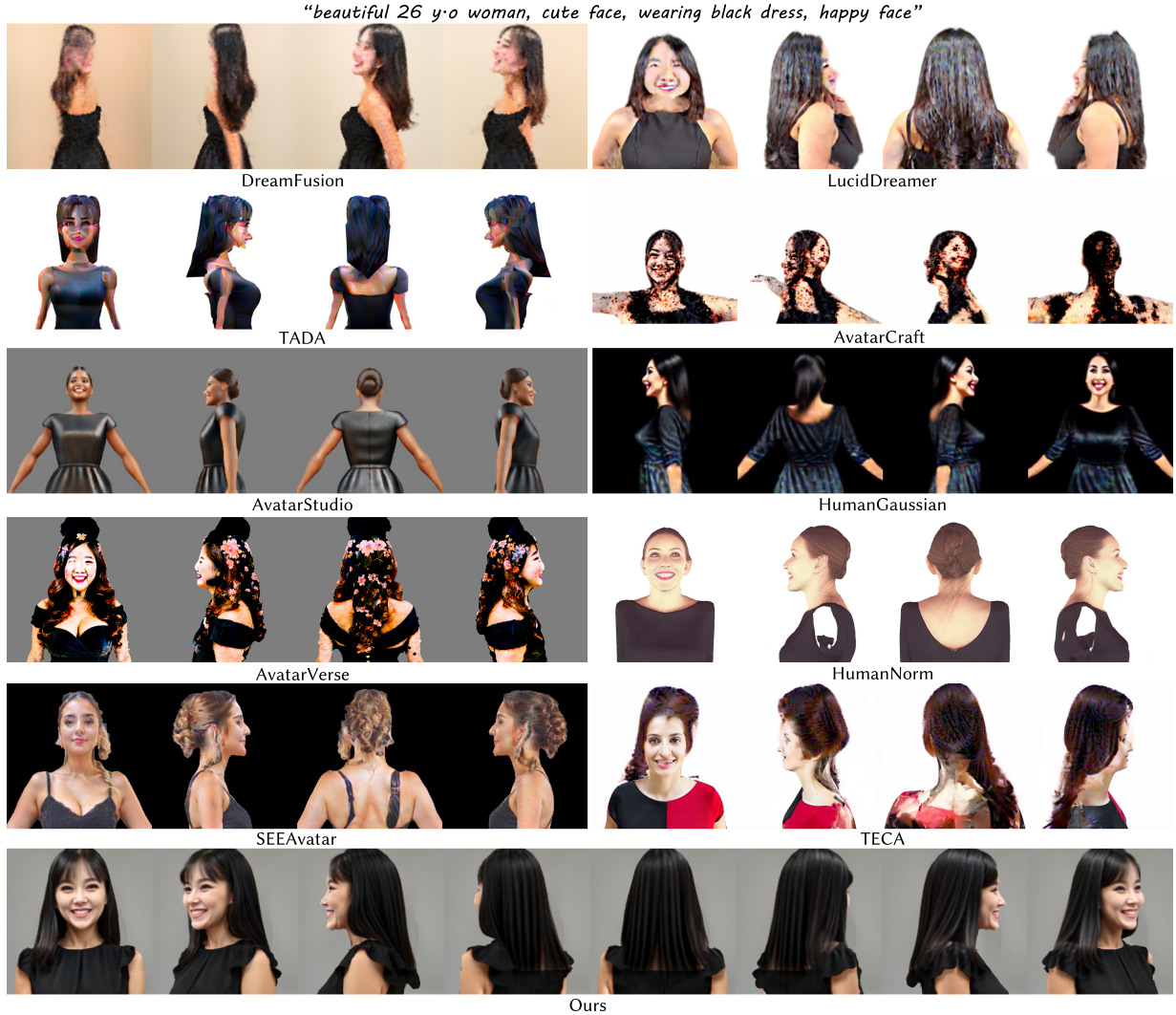


Fig. 5. Qualitative comparison to SOTA text-to-3D approaches: DreamFusion [Poole et al. 2023], LucidDreamer [Liang et al. 2023], TADA [Liao et al. 2023], AvatarCraft [Jiang et al. 2023], AvatarStudio [Zhang et al. 2023c], HumanGaussian [Liu et al. 2023b], AvatarVerse [Zhang et al. 2023a], HumanNorm [Huang et al. 2023a], SEEAvatar [Xu et al. 2023b], TECA [Zhang et al. 2024], and our method. The input prompt is presented at the top.

2023b], AvatarVerse [Zhang et al. 2023a], HumanNorm [Huang et al. 2023a], SEEAvatar [Xu et al. 2023b] and TECA [Zhang et al. 2024].

5.1 Qualitative Comparison

As shown in Fig. 5, we present a qualitative comparison between the SOTA methods and ours. To concentrate on the upper body region, we cropped some full-body results.

The outputs from DreamFusion and AvatarCraft display the Janus problem. LucidDreamer generates distorted geometry. TADA generates distorted and over-saturated results, lacking in realism. Both AvatarStudio and HumanGaussian fall short in terms of detail, suffering from unrealistic geometry and appearance. AvatarVerse produces unrealistic geometry and appearances. TECA does not generate the black dress in the input prompt and produces an unnatural

hairstyle. In contrast, our Portrait3D demonstrates superior performance in terms of result quality, generating high-quality and realistic 3D portraits. Furthermore, when compared to methods that represent 3D portraits using meshes and textures (such as TADA, AvatarVerse, HumanNorm, and SEEAvatar), our neural rendering-based framework produces more realistic results and exhibits the capability to represent complex shapes and materials.

5.2 Quantitative Comparison

We conducted a user study to quantitatively compare our Portrait3D to SOTA alternatives. We asked 20 participants to evaluate videos rendered from the 3D portraits generated by different methods and assign scores (ranging from 1 to 5) to those videos based on two criteria: overall quality and alignment with the input prompt.

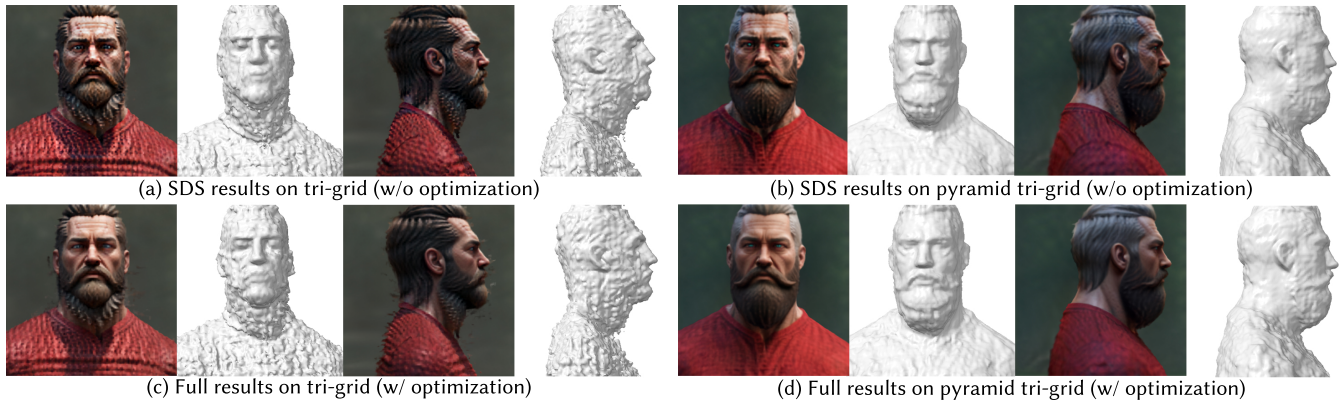


Fig. 6. The *pyramid tri-grid* is crucial for alleviating the “grid-like” artifacts. We showcase renderings of results obtained utilizing the two 3D representations (w/ and w/o optimization), accompanied by shapes extracted using Marching Cubes.

Table 1. Quantitative comparison results. The results with color ■ are derived from 25 distinct input prompts, while those with color ■ are derived from a single input prompt due to the inaccessibility of some methods.

Method	Quality \uparrow (User Study)		Alignment \uparrow (User Study)		FID \downarrow	CLIP Score \uparrow		
DreamFusion	1.10	1.35	1.54	2.95	285.5	336.2	0.61	0.76
LucidDreamer	2.28	1.75	3.36	2.85	202.5	182.6	0.65	0.67
TADA	2.57	1.35	3.24	2.45	197.2	180.5	0.68	0.68
AvatarCraft	1.25	1.05	1.40	1.75	248.9	341.8	0.57	0.51
HumanGaussian	3.30	3.40	3.66	3.85	203.9	214.4	0.73	0.66
HumanNorm	3.41	3.70	2.90	3.70	163.1	161.8	0.67	0.71
AvatarStudio	N/A	3.10	N/A	3.70	N/A	204.6	N/A	0.71
AvatarVerse	N/A	1.80	N/A	2.40	N/A	211.4	N/A	0.71
SEEAavatar	N/A	3.45	N/A	4.15	N/A	195.0	N/A	0.74
TECA	N/A	2.40	N/A	1.95	N/A	169.9	N/A	0.71
Ours	4.77	4.75	4.69	4.90	110.6	148.5	0.80	0.74

Moreover, the quality of the rendered views is further evaluated using the Fréchet Inception Distance (FID) [Heusel et al. 2017] by comparing the distribution’s distance between images generated by the diffusion model and rendered views. Additionally, we use the CLIP Score [Hessel et al. 2021] to quantify the semantic alignment between the prompts and the rendered views. For more details on quantitative experiments, please refer to the supplementary file.

Tab. 1 presents the average scores of DreamFusion, LucidDreamer, TADA, AvatarCraft, HumanGaussian, HumanNorm and ours across 25 different prompts. As the codes for AvatarStudio, AvatarVerse, SEEAavatar, and TECA are not publicly accessible, we also compare these methods with ours and other open-source ones using a single prompt (the one in Fig. 5).

The results of user studies, FID, and CLIP Score demonstrate that Portrait3D outperforms both general object generation and 3D avatar generation methods, achieving the highest overall result quality and the most accurate alignment with the prompt’s semantics. Notably, DreamFusion achieves a greater CLIP Score when assessed with a single prompt, largely due to its Janus problem in that case (as illustrated in Fig. 5). This issue leads most of its rendered view to better align with the “face” term in the input prompt.

6 ABLATION STUDY

6.1 Pyramid Tri-grid

In Sec. 3.2, we discussed the limitation of employing *tri-grid*, as it generates a noticeable “grid-like” artifact in the outputs. This effect is depicted in Fig. 6, using the same input prompt across all instances.

Following the generation method in Sec. 3.4, we use 3DPortraitGAN (which utilizes the *tri-grid* representation) to provide prior, as displayed in Fig. 6 (a). Subsequently, to illustrate the impact of using *tri-grid* in the final results, we apply the optimization process outlined in Sec. 3.5 to the SDS results on *tri-grid*. This is demonstrated in Fig. 6 (c). To ensure a fair comparison, we trained a new instance of 3DPortraitGAN that generates a *pyramid tri-grid* with resolutions {8, 16, 32, 64, 128, 256}, ensuring alignment with the *tri-grid* in 3DPortraitGAN (with a resolution of 256). Fig. 6 (b) illustrates the SDS results obtained using *pyramid tri-grid*. The optimization process is also applied to display the final results with our *pyramid tri-grid* in Fig. 6 (d).

The comparison reveals that using the *tri-grid* results in a grid-like texture, particularly noticeable on the T-shirt. This artifact is even preserved in the final results after employing the optimization process. In contrast, our *pyramid tri-grid* delivers a smoother, more realistic rendering with significantly reduced noise.

6.2 GANs Prior and Optimization

The effectiveness of our GANs prior and optimization strategy is demonstrated in Fig. 7. The Janus problem occurs when SDS is applied directly to a randomly initialized *pyramid tri-grid* without GANs prior and optimization (Fig. 7 (a)). Applying the GANs prior without optimization (Fig. 7 (b)) results in an unnatural color in the outputs. The results of our full method are generated using both GANs prior and optimization (Fig. 7 (c)), displaying improved realism in geometry and appearance.

7 DISCUSSION

Despite its notable performance, our method does have limitations.

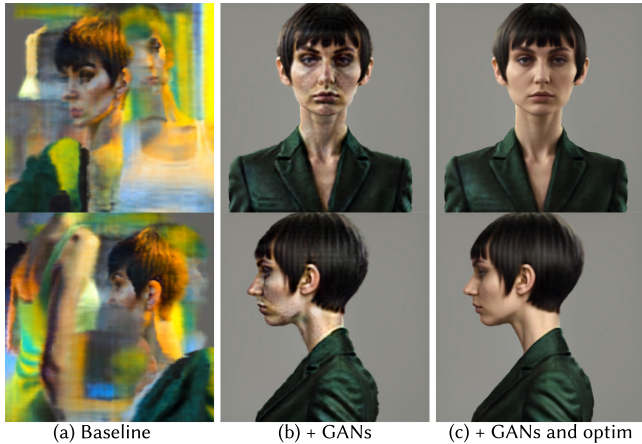


Fig. 7. Comparison of 3D portraits generated (a) without GANs prior and optimization (baseline), (b) with GANs prior but without optimization, and (c) with both GANs prior and optimization (our complete method).

Firstly, some 3D portraits generated by our 3DPortraitGAN aren’t entirely canonical due to the inversion method. These distortions won’t be rectified during text-to-3D-portraits generation and are evident in the final results (see samples in Fig. 8 (a)). This issue can be addressed by imposing additional constraints.

Secondly, certain semantic attributes of the background in the input prompt can influence the final result. As shown in the samples in Fig. 8 (b), the inclusion of “snow mountain background” in the input prompt results in unexpected snow appearing on the hair.

Thirdly, some of our results still grapple with semantic inconsistency. For instance, as seen in the samples in Fig. 8 (c), the man appears to be wearing a T-shirt from a frontal view, but seems to be wearing a vest from a rear view. This issue could potentially be addressed by employing a back-appearance hallucinator.

Fourthly, Portrait3D may generate inaccurate geometry, as illustrated in Fig. 8 (d). The girl’s braid is hardcoded as texture, yet it isn’t accurately represented in the geometry. This issue could potentially be addressed by incorporating a more robust geometry-aware diffusion model, such as HyperHuman [Liu et al. 2023a].

Moreover, Portrait3D is constrained to generating results that only include the head, neck, and shoulders. This limitation is imposed by the training dataset and the structure of 3DPortraitGAN. This constraint could potentially be overcome by employing a 3D full-body generator in the future.

Finally, some of our results still exhibit grid artifacts. We empirically identified a trade-off between the richness of detail in our results and the reduction of grid-like artifacts. We discovered that a higher learning rate for the high-resolution *tri-grid* within our *pyramid tri-grid* exacerbated the grid-like artifacts, while a lower learning rate resulted in blurrier results. To achieve a balance, we choose an appropriate learning rate (detailed in the supplementary material) that preserves details and subsequently use the optimization process to eliminate any remaining artifacts.

While not constituting a technical constraint, the high-quality 3D portraits produced by our Portrait3D could potentially engender



Fig. 8. Some failure cases of Portrait3D: (a) Distortions, (b) unexpected snow, (c) semantic inconsistency, and (d) incorrect geometry.

ethical concerns. We would like to underscore the importance of considering the potential ethical implications associated with realistic 3D portrait generation. The utilization of our method for the generation of realistic 3D portraits of a specific individual should be contingent on obtaining consent from the respective individual.

8 CONCLUSION

This paper presented Portrait3D, an innovative text-to-3D-portrait framework that utilizes the robust prior information provided by 3D-aware GANs. We began by training a 3D portrait generator capable of producing 360° canonical 3D portraits while incorporating a novel 3D representation to circumvent the interference of exclusive high-frequency information. Then, drawing from the prior information of the 3D portrait generator, given a text prompt, we initially project a randomly generated image aligned with the prompt into our 3D portrait generator’s latent space. The resulting latent code is used to synthesize a 3D representation. Subsequently, we distill the knowledge of the diffusion model into the 3D representation through score distillation sampling. To further enhance the quality of the 3D portrait, we apply the diffusion model to process the rendered images of the 3D portrait. The improved rendered images are then used as training data to optimize the 3D representation. We perceive our work as an exciting step forward in the domain of 3D portrait generation, and we hope it will inspire future research in areas such as talking heads and 3D avatar reconstruction.

REFERENCES

- Badour Albahar, Shunsuke Saito, Hung-Yu Tseng, Changil Kim, Johannes Kopf, and Jia-Bin Huang. 2023. Single-Image 3D Human Digitization with Shape-Guided Diffusion. In *SIGGRAPH Asia 2023 Conference Papers*. Article 62, 11 pages.
- Thiemo Alldieck, Hongyi Xu, and Cristian Sminchisescu. 2021. imGHUM: Implicit Generative Models of 3D Human Shape and Articulated Pose. In *Proceedings of the IEEE/CVF International Conference on Computer Vision (ICCV)*. 5461–5470.
- Sizhe An, Hongyi Xu, Yichun Shi, Guoxian Song, Umit Y. Ogras, and Linjie Luo. 2023. PanoHead: Geometry-Aware 3D Full-Head Synthesis in 360deg. In *IEEE/CVF Conference on Computer Vision and Pattern Recognition, CVPR*. 20950–20959.
- Eric R. Chan, Connor Z. Lin, Matthew A. Chan, Koki Nagano, Boxiao Pan, Shalini De Mello, Orazio Gallo, Leonidas J. Guibas, Jonathan Tremblay, Sameh Khamis, Tero Karras, and Gordon Wetzstein. 2022. Efficient Geometry-aware 3D Generative Adversarial Networks. In *IEEE/CVF Conference on Computer Vision and Pattern Recognition, CVPR*. 16102–16112.

- Eric R. Chan, Marco Monteiro, Petr Kellnhofer, Jiajun Wu, and Gordon Wetzstein. 2021. Pi-GAN: Periodic Implicit Generative Adversarial Networks for 3D-Aware Image Synthesis. In *IEEE Conference on Computer Vision and Pattern Recognition, CVPR*. 5799–5809.
- Xingyu Chen, Yu Deng, and Baoyuan Wang. 2023a. Mimic3D: Thriving 3D-Aware GANs via 3D-to-2D Imitation. In *Proceedings of the IEEE/CVF International Conference on Computer Vision (ICCV)*. 2338–2348.
- Yufan Chen, Lizhen Wang, Qijing Li, Hongjiang Xiao, Shengping Zhang, Hongxun Yao, and Yebin Liu. 2023b. MonoGaussianAvatar: Monocular Gaussian Point-based Head Avatar. *CoRR* abs/2312.04558 (2023).
- Jun Gao, Tianchang Shen, Zian Wang, Wenzheng Chen, Kangxue Yin, Daiqing Li, Or Litany, Zan Gojcic, and Sanja Fidler. 2022. GET3D: A Generative Model of High Quality 3D Textured Shapes Learned from Images. In *Advances in Neural Information Processing Systems*, Vol. 35. 31841–31854.
- Ian J. Goodfellow, Jean Pouget-Abadie, Mehdi Mirza, Bing Xu, David Warde-Farley, Sherjil Ozair, Aaron C. Courville, and Yoshua Bengio. 2014. Generative Adversarial Nets. In *Advances in Neural Information Processing Systems*, Vol. 27. 2672–2680.
- Jiatao Gu, Lingjie Liu, Peng Wang, and Christian Theobalt. 2022. StyleNeRF: A Style-based 3D Aware Generator for High-resolution Image Synthesis. In *The 10th International Conference on Learning Representations, ICLR*.
- Riza Alp Güler, Natalia Neverova, and Iasonas Kokkinos. 2018. DensePose: Dense Human Pose Estimation in the Wild. In *IEEE/CVF Conference on Computer Vision and Pattern Recognition, CVPR*. 7297–7306.
- Ishaan Gulrajani, Faruk Ahmed, Martin Arjovsky, Vincent Dumoulin, and Aaron C. Courville. 2017. Improved Training of Wasserstein GANs. In *Advances in Neural Information Processing Systems*, Vol. 30. 5767–5777.
- Xiao Han, Yukang Cao, Kai Han, Xiatian Zhu, Jiankang Deng, Yi-Zhe Song, Tao Xiang, and Kwan-Yee K. Wong. 2023. HeadSculpt: Crafting 3D Head Avatars with Text. *CoRR* abs/2306.03038 (2023).
- Ayaan Haque, Matthew Tancik, Alexei A. Efros, Aleksander Holynski, and Angjoo Kanazawa. 2023. Instruct-NeRF2NeRF: Editing 3D Scenes with Instructions. In *IEEE/CVF International Conference on Computer Vision, ICCV 2023, Paris, France, October 1-6, 2023*. IEEE, 19683–19693.
- Jack Hessel, Ari Holtzman, Maxwell Forbes, Ronan Le Bras, and Yejin Choi. 2021. CLIPScore: A Reference-free Evaluation Metric for Image Captioning. In *Proceedings of the 2021 Conference on Empirical Methods in Natural Language Processing, EMNLP*. 7514–7528.
- Martin Heusel, Hubert Ramsauer, Thomas Unterthiner, Bernhard Nessler, and Sepp Hochreiter. 2017. GANs Trained by a Two Time-Scale Update Rule Converge to a Local Nash Equilibrium. In *Advances in Neural Information Processing Systems*, Vol. 30. 6626–6637.
- Hsuan-I Ho, Jie Song, and Otmar Hilliges. 2023. SiTH: Single-view Textured Human Reconstruction with Image-Conditioned Diffusion. [arXiv:2311.15855 \[cs.CV\]](https://arxiv.org/abs/2311.15855)
- Jonathan Ho, Ajay Jain, and Pieter Abbeel. 2020. Denoising Diffusion Probabilistic Models. In *Advances in Neural Information Processing Systems*, Vol. 33. 6840–6851.
- Shoukang Hu, Fangzhou Hong, Tao Hu, Liang Pan, Haiyi Mei, Weiye Xiao, Lei Yang, and Ziwei Liu. 2023. HumanLiff: Layer-wise 3D Human Generation with Diffusion Model. *CoRR* abs/2308.09712 (2023).
- Xin Huang, Ruizhi Shao, Qi Zhang, Hongwen Zhang, Ying Feng, Yebin Liu, and Qing Wang. 2023a. HumanNorm: Learning Normal Diffusion Model for High-quality and Realistic 3D Human Generation. *CoRR* abs/2310.01406 (2023).
- Yangyi Huang, Hongwei Yi, Yuliang Xiu, Tingting Liao, Jiaxiang Tang, Deng Cai, and Justus Thies. 2023b. [arXiv:2308.08545 \[cs.CV\]](https://arxiv.org/abs/2308.08545)
- Ruixiang Jiang, Can Wang, Jingbo Zhang, Menglei Chai, Mingming He, Dongdong Chen, and Jing Liao. 2023. AvatarCraft: Transforming Text into Neural Human Avatars with Parameterized Shape and Pose Control. In *Proceedings of the IEEE/CVF International Conference on Computer Vision (ICCV)*. 14371–14382.
- Tero Karras, Timo Aila, Samuli Laine, and Jaakko Lehtinen. 2018. Progressive Growing of GANs for Improved Quality, Stability, and Variation. In *6th International Conference on Learning Representations, ICLR*.
- Bernhard Kerbl, Georgios Kopanas, Thomas Leimkuehler, and George Drettakis. 2023a. 3D Gaussian Splatting for Real-Time Radiance Field Rendering. *ACM Trans. Graph.* 42, 4 (2023), 139:1–139:14.
- Bernhard Kerbl, Georgios Kopanas, Thomas Leimkuehler, and George Drettakis. 2023b. 3D Gaussian Splatting for Real-Time Radiance Field Rendering. *ACM Trans. Graph.* 42, 4 (2023), 139:1–139:14.
- Jaehoon Ko, Kyuson Cho, Daewon Choi, Kwangrok Ryo, and Seungryong Kim. 2023. 3D GAN Inversion with Pose Optimization. In *IEEE/CVF Winter Conference on Applications of Computer Vision, WACV 2023, Waikoloa, HI, USA, January 2-7, 2023*. 2966–2975.
- Nikos Kolotouros, Thiemo Alldieck, Andrei Zanfir, Eduard Gabriel Bazavan, Mihai Fieraru, and Cristian Sminchisescu. 2023. DreamHuman: Animatable 3D Avatars from Text. *CoRR* abs/2306.09329 (2023).
- Tianye Li, Timo Bolkart, Michael J. Black, Hao Li, and Javier Romero. 2017. Learning a model of facial shape and expression from 4D scans. *ACM Trans. Graph.* 36, 6 (2017), 194:1–194:17.
- Yixun Liang, Xin Yang, Jiantao Lin, Haodong Li, Xiaogang Xu, and Yingcong Chen. 2023. LucidDreamer: Towards High-Fidelity Text-to-3D Generation via Interval Score Matching. *CoRR* abs/2311.11284 (2023).
- Tingting Liao, Hongwei Yi, Yuliang Xiu, Jiaxiang Tang, Yangyi Huang, Justus Thies, and Michael J. Black. 2023. TADA! Text to Animatable Digital Avatars. *CoRR* abs/2308.10899 (2023).
- Xian Liu, Jian Ren, Aliaksandr Siarohin, Ivan Skorokhodov, Yanyu Li, Dahua Lin, Xihui Liu, Ziwei Liu, and Sergey Tulyakov. 2023a. HyperHuman: Hyper-Realistic Human Generation with Latent Structural Diffusion. *CoRR* abs/2310.08579 (2023).
- Xian Liu, Xiaohang Zhan, Jiaxiang Tang, Ying Shan, Gang Zeng, Dahua Lin, Xihui Liu, and Ziwei Liu. 2023b. HumanGaussian: Text-Driven 3D Human Generation with Gaussian Splatting. *CoRR* abs/2311.17061 (2023).
- Matthew Loper, Naureen Mahmood, Javier Romero, Gerard Pons-Moll, and Michael J. Black. 2015. SMPL: a skinned multi-person linear model. *ACM Trans. Graph.* 34, 6 (2015), 248:1–248:16.
- Ben Mildenhall, Pratul P. Srinivasan, Matthew Tancik, Jonathan T. Barron, Ravi Ramamoorthi, and Ren Ng. 2020. NeRF: Representing Scenes as Neural Radiance Fields for View Synthesis. In *Computer Vision - ECCV 2020 - 16th European Conference, Glasgow, UK, August 23-28, 2020, Proceedings, Part I (Lecture Notes in Computer Science, Vol. 12346)*. 405–421.
- Thomas Müller, Alex Evans, Christoph Schied, and Alexander Keller. 2022. Instant neural graphics primitives with a multiresolution hash encoding. *ACM Trans. Graph.* 41, 4 (2022), 102:1–102:15.
- Thu H Nguyen-Phuoc, Christian Richardt, Long Mai, Yongliang Yang, and Niloy Mitra. 2020. BlockGAN: Learning 3D Object-aware Scene Representations from Unlabelled Images. In *Advances in Neural Information Processing Systems*, Vol. 33. 6767–6778.
- Ben Poole, Ajay Jain, Jonathan T. Barron, and Ben Mildenhall. 2023. DreamFusion: Text-to-3D using 2D Diffusion. In *The 11th International Conference on Learning Representations, ICLR*.
- Alec Radford, Luke Metz, and Soumith Chintala. 2016. Unsupervised Representation Learning with Deep Convolutional Generative Adversarial Networks. In *4th International Conference on Learning Representations, ICLR*.
- Alfredo Rivero, ShahRukh Athar, Zhixin Shu, and Dimitris Samaras. 2024. Rig3DGS: Creating Controllable Portraits from Casual Monocular Videos. *CoRR* abs/2402.03723 (2024).
- Robin Rombach, Andreas Blattmann, Dominik Lorenz, Patrick Esser, and Björn Ommer. 2022. High-Resolution Image Synthesis With Latent Diffusion Models. In *Proceedings of the IEEE/CVF Conference on Computer Vision and Pattern Recognition (CVPR)*. 10684–10695.
- Katja Schwarz, Axel Sauer, Michael Niemeyer, Yiyi Liao, and Andreas Geiger. 2022. VoxGRAF: Fast 3D-Aware Image Synthesis with Sparse Voxel Grids. In *Advances in Neural Information Processing Systems*, Vol. 35. 33999–34011.
- Ivan Skorokhodov, Sergey Tulyakov, Yiqun Wang, and Peter Wonka. 2022. EpiGRAF: Rethinking training of 3D GANs. *CoRR* abs/2206.10535 (2022). <https://doi.org/10.48550/arXiv.2206.10535> [arXiv:2206.10535](https://arxiv.org/abs/2206.10535)
- Jingxiang Sun, Xuan Wang, Lizhen Wang, Xiaoyu Li, Yong Zhang, Hongwen Zhang, and Yebin Liu. 2022. Next3D: Generative Neural Texture Rasterization for 3D-Aware Head Avatars. *CoRR* abs/2211.11208 (2022).
- Alex Trevisan, Matthew A. Chan, Michael Stengel, Eric R. Chan, Chao Liu, Zhiding Yu, Sameh Khamis, Manmohan Chandraker, Ravi Ramamoorthi, and Koki Nagano. 2023. Real-Time Radiance Fields for Single-Image Portrait View Synthesis. *ACM Trans. Graph.* 42, 4 (2023), 135:1–135:15.
- Alex Trevisan, Matthew A. Chan, Towaki Takikawa, Umar Iqbal, Shalini De Mello, Manmohan Chandraker, Ravi Ramamoorthi, and Koki Nagano. 2024. What You See is What You GAN: Rendering Every Pixel for High-Fidelity Geometry in 3D GANs. *CoRR* abs/2401.02411 (2024).
- Jie Wang, Jiu-Cheng Xie, Xianyan Li, Feng Xu, Chi-Man Pun, and Hao Gao. 2024. GaussianHead: High-fidelity Head Avatars with Learnable Gaussian Derivation. [arXiv:2312.01632 \[cs.CV\]](https://arxiv.org/abs/2312.01632)
- Peng Wang, Lingjie Liu, Yuan Liu, Christian Theobalt, Taku Komura, and Wenping Wang. 2021. NeuS: Learning Neural Implicit Surfaces by Volume Rendering for Multi-view Reconstruction. In *Advances in Neural Information Processing Systems*, Vol. 34. 27171–27183.
- Tengfei Wang, Bo Zhang, Ting Zhang, Shuyang Gu, Jianmin Bao, Tadas Baltrusaitis, Jingjing Shen, Dong Chen, Fang Wen, Qifeng Chen, and Baining Guo. 2023b. RODIN: A Generative Model for Sculpting 3D Digital Avatars Using Diffusion. In *Proceedings of the IEEE/CVF Conference on Computer Vision and Pattern Recognition (CVPR)*. 4563–4573.
- Zhengyi Wang, Cheng Lu, Yikai Wang, Fan Bao, Chongxuan Li, Hang Su, and Jun Zhu. 2023a. ProlificDreamer: High-Fidelity and Diverse Text-to-3D Generation with Variational Score Distillation. In *Advances in Neural Information Processing Systems*, Vol. 34.
- Yiqian Wu, Hao Xu, Xiangjun Tang, Hongbo Fu, and Xiaogang Jin. 2023a. 3DPortraitGAN: Learning One-Quarter Headshot 3D GANs from a Single-View Portrait Dataset with Diverse Body Poses. [arXiv:2307.14770 \[cs.CV\]](https://arxiv.org/abs/2307.14770)

- Yue Wu, Sicheng Xu, Jianfeng Xiang, Fangyun Wei, Qifeng Chen, Jiaolong Yang, and Xin Tong. 2023b. AniPortraitGAN: Animatable 3D Portrait Generation from 2D Image Collections. In *SIGGRAPH Asia 2023 Conference Papers, SA 2023, Sydney, NSW, Australia, December 12-15, 2023*, June Kim, Ming C. Lin, and Bernd Bickel (Eds.). ACM, 51:1–51:9.
- Jiaxin Xie, Hao Ouyang, Jingtian Piao, Chenyang Lei, and Qifeng Chen. 2023. High-fidelity 3D GAN Inversion by Pseudo-multi-view Optimization. In *IEEE/CVF Conference on Computer Vision and Pattern Recognition, CVPR 2023, Vancouver, BC, Canada, June 17-24, 2023*. IEEE, 321–331.
- Yuelang Xu, Benwang Chen, Zhe Li, Hongwen Zhang, Lizhen Wang, Zerong Zheng, and Yebin Liu. 2023a. Gaussian Head Avatar: Ultra High-fidelity Head Avatar via Dynamic Gaussians. *CoRR abs/2312.03029 (2023)*.
- Yuanyou Xu, Zongxin Yang, and Yi Yang. 2023b. SEEAAvatar: Photorealistic Text-to-3D Avatar Generation with Constrained Geometry and Appearance. [arXiv:2312.08889 \[cs.CV\]](https://arxiv.org/abs/2312.08889)
- Han Yi, Zhedong Zheng, Xiangyu Xu, and Tat-Seng Chua. 2023. Progressive Text-to-3D Generation for Automatic 3D Prototyping. *CoRR abs/2309.14600 (2023)*.
- Fei Yin, Yong Zhang, Xuan Wang, Tengfei Wang, Xiaoyu Li, Yuan Gong, Yanbo Fan, Xiaodong Cun, Ying Shan, Cengiz Öztireli, and Yujiu Yang. 2023. 3D GAN Inversion with Facial Symmetry Prior. In *IEEE/CVF Conference on Computer Vision and Pattern Recognition, CVPR 2023, Vancouver, BC, Canada, June 17-24, 2023*. IEEE, 342–351.
- Huichao Zhang, Bowen Chen, Hao Yang, Liao Qu, Xu Wang, Li Chen, Chao Long, Feida Zhu, Kang Du, and Min Zheng. 2023a. AvatarVerse: High-quality & Stable 3D Avatar Creation from Text and Pose. *CoRR abs/2308.03610 (2023)*.
- Hao Zhang, Yao Feng, Peter Kulits, Yandong Wen, Justus Thies, and Michael J. Black. 2024. TECA: Text-Guided Generation and Editing of Compositional 3D Avatars.
- Jianfeng Zhang, Xuanmeng Zhang, Huichao Zhang, Jun Hao Liew, Chenxu Zhang, Yi Yang, and Jiashi Feng. 2023c. AvatarStudio: High-fidelity and Animatable 3D Avatar Creation from Text. *CoRR abs/2311.17917 (2023)*.
- Xuanmeng Zhang, Jianfeng Zhang, Rohan Chacko, Hongyi Xu, Guoxian Song, Yi Yang, and Jiashi Feng. 2023b. GETAvatar: Generative Textured Meshes for Animatable Human Avatars. In *Proceedings of the IEEE/CVF International Conference on Computer Vision (ICCV)*, 2273–2282.
- Zhenglin Zhou, Fan Ma, Hehe Fan, and Yi Yang. 2024. HeadStudio: Text to Animatable Head Avatars with 3D Gaussian Splatting. *CoRR abs/2402.06149 (2024)*.
- Jun-Yan Zhu, Zhoutong Zhang, Chengkai Zhang, Jiajun Wu, Antonio Torralba, Josh Tenenbaum, and Bill Freeman. 2018. Visual Object Networks: Image Generation with Disentangled 3D Representations. In *Advances in Neural Information Processing Systems*, Vol. 31. 118–129.



Fig. 9. Examples of 3D portraits generated using Portrait3D.



Fig. 10. Examples of 3D portraits generated using Portrait3D.